

The Adsorption of Dyes in Chitin. III. Intraparticle Diffusion Processes

G. McKAY,* H. S. BLAIR, and J. GARDNER, *Department of Chemical Engineering, The Queen's University of Belfast, Belfast, BT9 5DL, Northern Ireland*

Synopsis

Intraparticle diffusion processes for the adsorption of dyestuffs onto chitin have been studied. The amount of dye adsorbed per gram of chitin has been plotted against the square root of time. The slope of this plot is linear and has been defined as a rate parameter k . This rate parameter has been determined for a number of process variables, including initial dye concentration, agitation, chitin particle size, chitin mass, temperature, and solution pH. However, sometimes two and even three linear regions are apparent on the root time plots indicating a possible branched pore mechanism. The controlling mechanisms are due to macropores and micropores in the chitin particle creating rapidly and slowly diffusing regions.

INTRODUCTION

The experimental results for the adsorption of various dyestuffs onto chitin have been reported in a previous paper.¹ Adsorption isotherms were undertaken and demonstrated that chitin had a high capacity to adsorb acidic dyes and could also adsorb substantial quantities of mordant and direct dyes. In an attempt to predict the kinetics of the adsorption processes² it was found that kinetic models based on external mass transfer only were inadequate to describe the variation in concentration with time after the initial five minutes. Consequently, it was concluded that a second resistance, operating over a much longer time scale, must be a major rate controlling factor.

The aim of this paper is to demonstrate these intraparticle diffusional effects and correlate them in terms of the system variables. The experimental apparatus and methodology has been reported previously.¹

Intraparticle Diffusion

The transport of adsorbates within the internal structure of adsorbents is usually described as either homogeneous solid phase diffusion or pore diffusion. In the homogeneous model, the adsorption process occurs at the outer surface of the particle initially, followed by diffusion of the adsorbate in the adsorbed state. The particle is assumed to be homogeneous, although it may still be used for particles with substantial porosity, and takes no account of surface area or pore size distribution. The pore diffusion model pictures the particles as consisting of a solid phase interspersed with very small pores. Various pore size distributions have been postulated and the sizes range from 1–2000 nm. The

* To whom correspondence should be addressed.

fraction of a particle which is porous is designated, the porosity, and ranges from 0, for a homogeneous nonporous solid, to 1, for no solid content at all.

The classical treatment of diffusion is attributed to Fick, and his second law

$$\frac{dC}{dt} = D \frac{d^2C}{dX^2} \quad (1)$$

is the fundamental differential equation for diffusion in an adsorbent where there is a concentration gradient along the X axis. The equation is modified for spherical particles.³

$$\frac{dC}{dt} = \frac{1}{r^2} \left(\frac{\partial}{\partial r} D r^2 \frac{\partial C}{\partial r} + \frac{1}{\sin \theta} \frac{\partial}{\partial \theta} D \sin \theta + \frac{D}{\sin^2 \theta} \frac{\partial^2 C}{\partial \phi^2} \right) \quad (2)$$

using the spherical coordinates r , θ , and ϕ .

The mathematical solution of the differential equations for unsteady diffusion has been performed for spheres subject to particular boundary equations. The model assumes (i) the concentration of solute is uniform at C_0 and is zero in the adsorbent particle at $t = 0$; (ii) diffusion is radial with no variation in concentration with angular position; and (iii) the resistance to transfer in the medium surrounding the particle is significant only in the early stages of diffusion. One solution⁴ indicates a linear relationship between $(C_0 - C_t)/(C_0 - C_e)$ and $(Dt/r^2)^{0.5}$ for much of the adsorption process. Since D and r are constant for a given system then the amount adsorbed Y_t , which is proportional to $(C_0 - C_t)/(C_0 - C_e)$, will be linearly dependent on $t^{0.5}$. The boundary condition (iii) allows an initial curved portion due to surface effects, and the intraparticle diffusion is generally held to predominate over the 10–60% adsorption range with a decreasing rate of diffusion (due to bulk solute concentration and surface solute concentration decreases), producing another curved portion, leading eventually to an equilibrium plateau. The slope of the Y_t vs. $t^{0.5}$ linear section is designated k and is used as a rate parameter. This parameter, although strictly not a reaction rate, has been correlated with several of the system parameters such as C_0 , d_p , etc. to characterize the influence of intraparticle diffusion.⁵

DISCUSSION

A plot of Y_t vs. $t^{0.5}$ reveals the extent of intraparticle diffusion influence in the adsorption mechanism and comparison of rate parameter k values indicates how the rate of the adsorption, occurring under this resistance, varies as the system conditions are varied. The first observation which the results revealed was the occurrence of up to three separate linear portions of the plots (and also a linear desorption region for those systems which underwent desorption—see Fig. 7). This type of behavior has been alluded to in the literature,⁶ although the authors, Bell and Molof, identified linear sections in modified Y_t vs. t plots. They explained their results by postulating different adsorption rates due to stepwise transport through the pore size ranges suggested by Dubinin.⁷ This explanation appears reasonable in view of the results reported here. Table I lists the rate parameters, k_1 corresponding to the first linear section of the Y_t vs. $t^{0.5}$ plots.

Several classifications of pore size distributions in porous solids exist, but the

TABLE I
Rate Parameter k , Values ($\text{mg} \cdot \text{G}^{-1} \cdot \text{min}^{0.5}$)^a

Variable	AB 25	Dye AB 158	MY 5	DR 84
<i>Concn (ppm)</i>				
50	6.61	5.09	—	—
100	7.28	7.68	10.00	0.97
150	6.62	7.82	9.69	1.26
200	5.52	9.66	10.00	1.52
250	6.46	9.12	9.58	1.87
300	6.73	10.00	—	1.91
<i>Agitation (rpm)</i>				
200	7.12	9.17	11.88	1.26
300	6.15	8.35	7.83	1.67
500	6.25	9.83	6.86	1.36
600	6.27	9.22	6.15	1.32
<i>Particle size (μ)</i>				
302	7.95	20.65	10.31	2.16
427	5.96	12.22	11.14	1.79
780	4.68	7.08	7.32	1.25
925	3.96	6.04	7.20	1.23
<i>Mass (g)</i>				
0.4	4.26	7.54	—	—
0.7	4.31	8.42	—	—
1.2	4.59	9.04	—	—
1.5	5.18	8.58	—	—
2.5	—	—	14.47	1.48
5.0	6.20	7.22	9.58	1.52
7.5	—	—	8.72	1.23
<i>Temp ($^{\circ}\text{C}$)</i>				
30	9.73	5.36	8.33	1.73
40	11.50	7.34	7.45	1.88
50	17.25	4.71	11.00	2.13
<i>pH</i>				
2.0	22.50	10.84	—	—
7.0	3.62	6.77	—	—
9.0	4.48	3.37	—	—

^a AB 25 = Telon Blue (Acid Blue 25); AB 158 = Neolan Blue 2G (Acid Blue 158); MY 5 = Eriochrome Flavine A (Mordant Yellow 5); DR 84 = Solophenyl Brown 3RL (Directed Red 84).

classification proposed by Dubinin breaks pores down into three size groupings: micropores with radius 1–2 nm, transitional pores with radius 2–100 nm, and macropores with radius 100–2000 nm. The distribution of these sizes will also affect the extent of adsorption.

Effect of Initial Concentration

The effect of initial concentration on the k_1 values for AB 25 is shown in Figure 1. The k_1 values were derived from the gradients of the first linear sections, and, as can be seen, these sections were almost perfectly parallel, indicating a constancy in the k_1 values. The initial concentration therefore appeared to have no significant influence on the intraparticle diffusion rates for this dye. This behavior was repeated with MY 5 but both DR 84 and AB 158 showed an in-

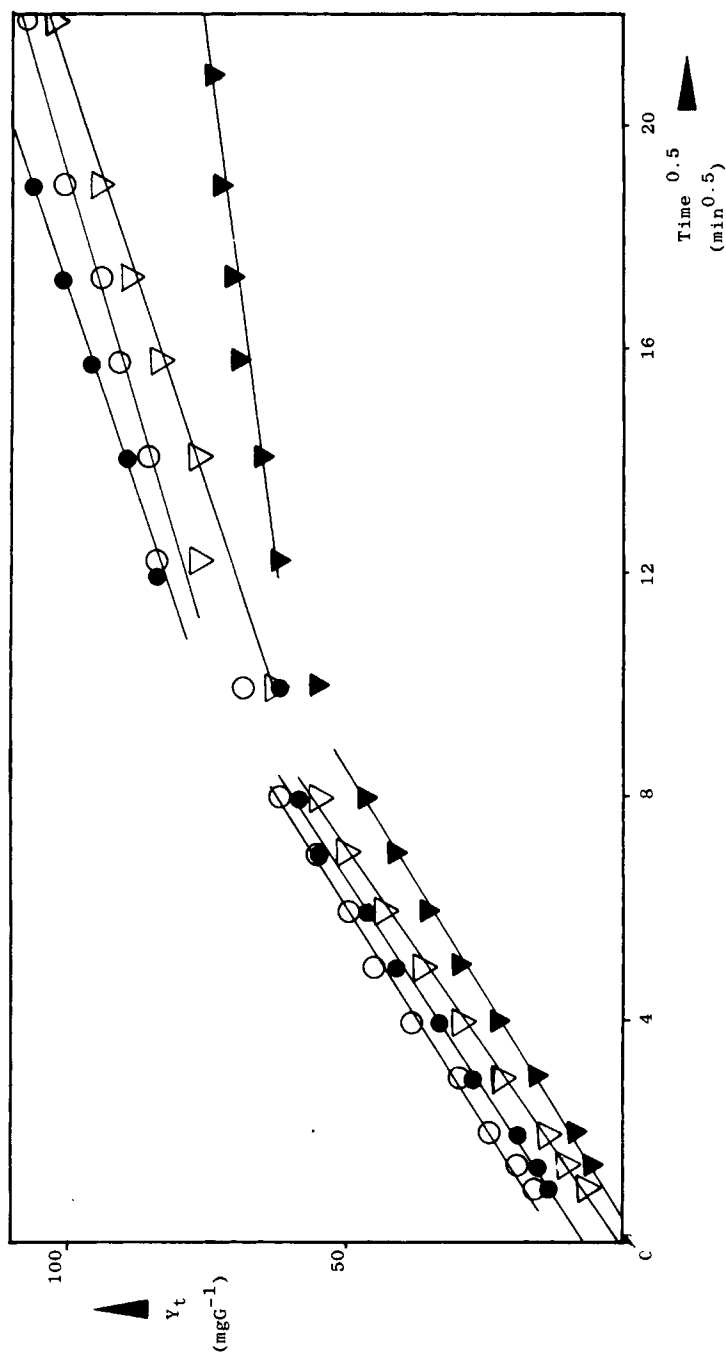


Fig. 1. Intraparticle diffusion dependence for AB 25 (concentration): (∇) 100 ppm; (\blacktriangledown) 50 ppm; (\circ) 150 ppm; (\bullet) 250 ppm.

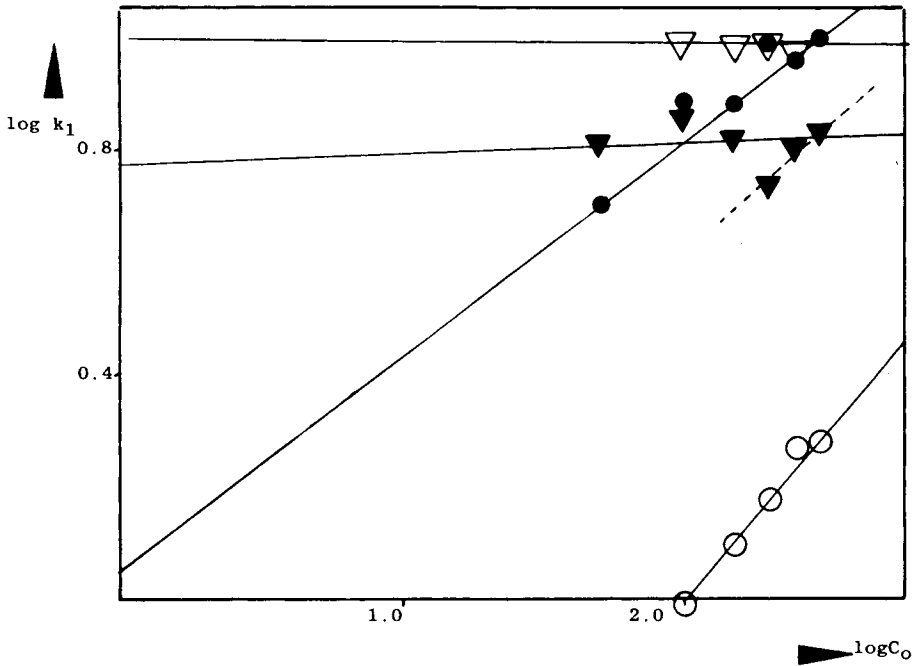


Fig. 2. Variation of $\log k_1$ with $\log C_0$ for the four dyes: (∇) MY 5; (\blacktriangledown) AB 25; (\circ) DR 84; (\bullet) AB 158.

creasing trend with concentration. The theoretical equations for intraparticle diffusion indicate that the concentration dependence of a diffusion-adsorption process will vary depending on the characteristics of the adsorption isotherm and on the fraction of solute adsorbed at equilibrium. In the case of intraparticle diffusion being the only rate-determining step it was found that k_1 varied with the square root of the initial concentrations used.⁵ In the logarithm plot of k_1 vs. C_0 in Figure 2 the exponents of

$$k_1 \propto C_0^n \tag{3}$$

were found and are listed in Table II. With the exception of the MY 5 value and the value for all C_0 values for AB 25, n did center around the 0.5 value, confirming that intraparticle diffusion was a prominent factor in the adsorption process.

TABLE II
Exponent n Values for Eqs. (6.12) and (6.13)

Dye	Exponent n	
	Eq. (3)	Eq. (4)
AB 25	0.02	0.55
AB 25 ^a	0.44	—
AB 158	0.39	1.06
MY 5	0.00	0.59
DR 84	0.59	0.49

^a High C_0 values.

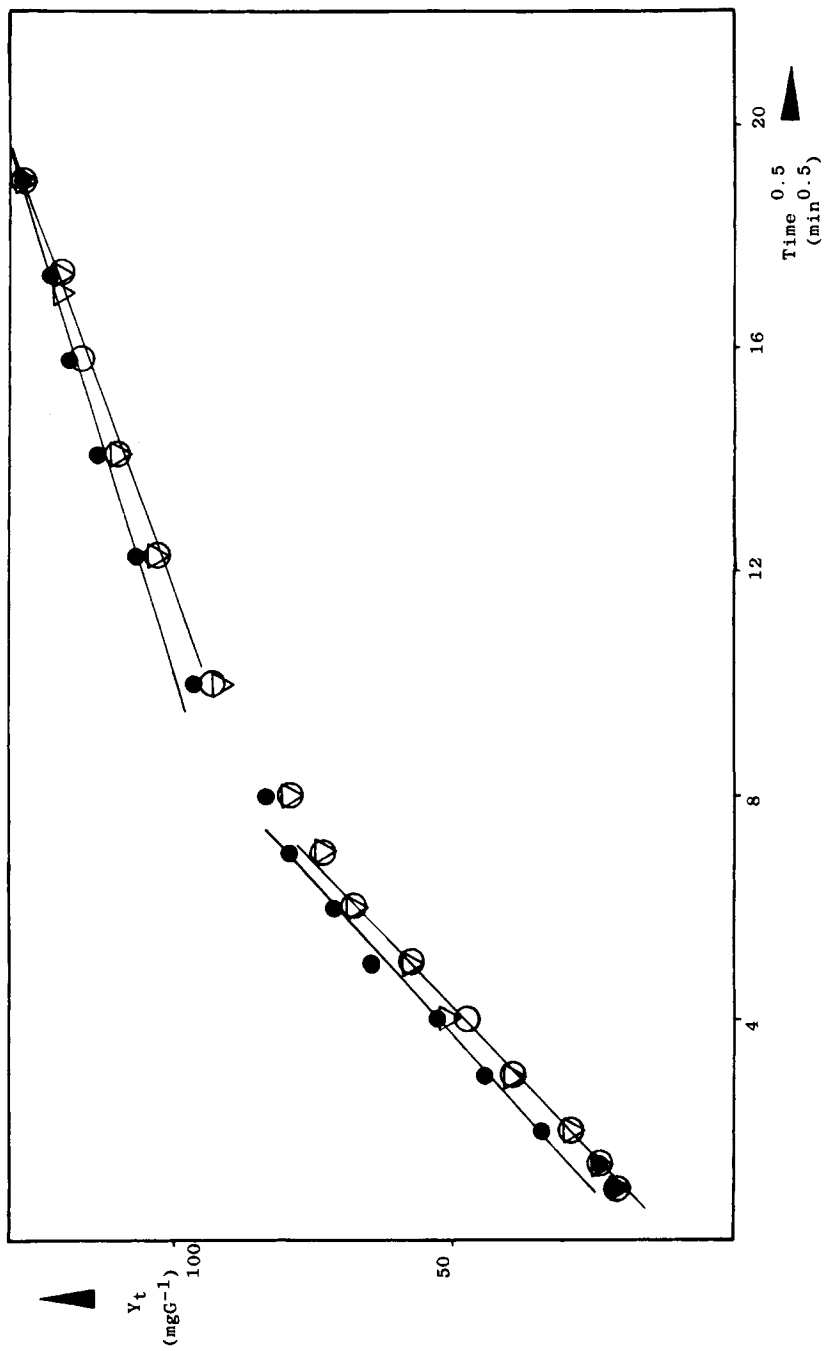


Fig. 3. Intraparticle diffusion dependence for AB 158 (agitation): (∇) 200 rpm; (\bullet) 600 rpm; (\circ) 400 rpm.

Effect of Agitation

The effect of agitation on the k_1 values for AB 158 is represented in Figure 3. Again, a constancy in magnitude was observed, and this was largely reflected in the studies for the other dyes. This result was not unexpected since it was noted earlier that the effect of agitation would be mainly significant in surface mass transfer treatments.

Effect of Particle Size

The effect of particle size on the k_1 values for DR 84 is shown in Figure 4. Table I shows that each of the dyes gave a decrease in the k_1 values as the particle size was increased. In most cases the decrease was gradual, but AB 158 showed a fairly steep decrease. Weber and Morris⁵ have shown that if surface mass transfer is a prominent resistance in the adsorption, then k_1 should vary with the reciprocal of particle diameter. Figure 5 shows how the exponents n were determined for the equation

$$k_1 \propto 1/(d_p)^n$$

for each of the four dyes. The values of n are listed in Table II and show that the n values centered around a value of 0.55, which is usually interpreted as an indication of intraparticle diffusion predominance in the adsorption mechanism. The apparently anomalous value of 1.06 for B 158, which suggests surface mass transfer as being the significant resistance, must be considered alongside the results, already discussed, for the surface mass transfer treatments.² These showed conclusively that surface mass transfer was not the predominant resistance; therefore, this result is better interpreted in terms of the physical resistance offered by restricting the area of surface available for initial adsorption, which, as a consequence, reduced the amount of dye available for intraparticle diffusion.

Effect of Chitin Mass

The effect of mass on the k_1 values for MY 5 is shown in Figure 5. Table I shows that only MY 5 showed any significant variation in k_1 values, but Figure 4 demonstrates the level of error in fixing the initial slopes for this dye. Overall there was not a significant variation in k_1 with mass.

Effect of Temperature

The effect of temperature on the k_1 values for AB 25 is shown on Figure 6. Table I shows how the values varied for all four dyes. The results, with the exception of AB 158, behaved as expected, showing an increased rate as the temperature increased. This lack of temperature effect is probably linked to the fact that chelation plays an important part in the adsorption of AB 158 on chitin due to the presence of Cr^{3+} , the chelating reaction not being particularly influenced by temperature.

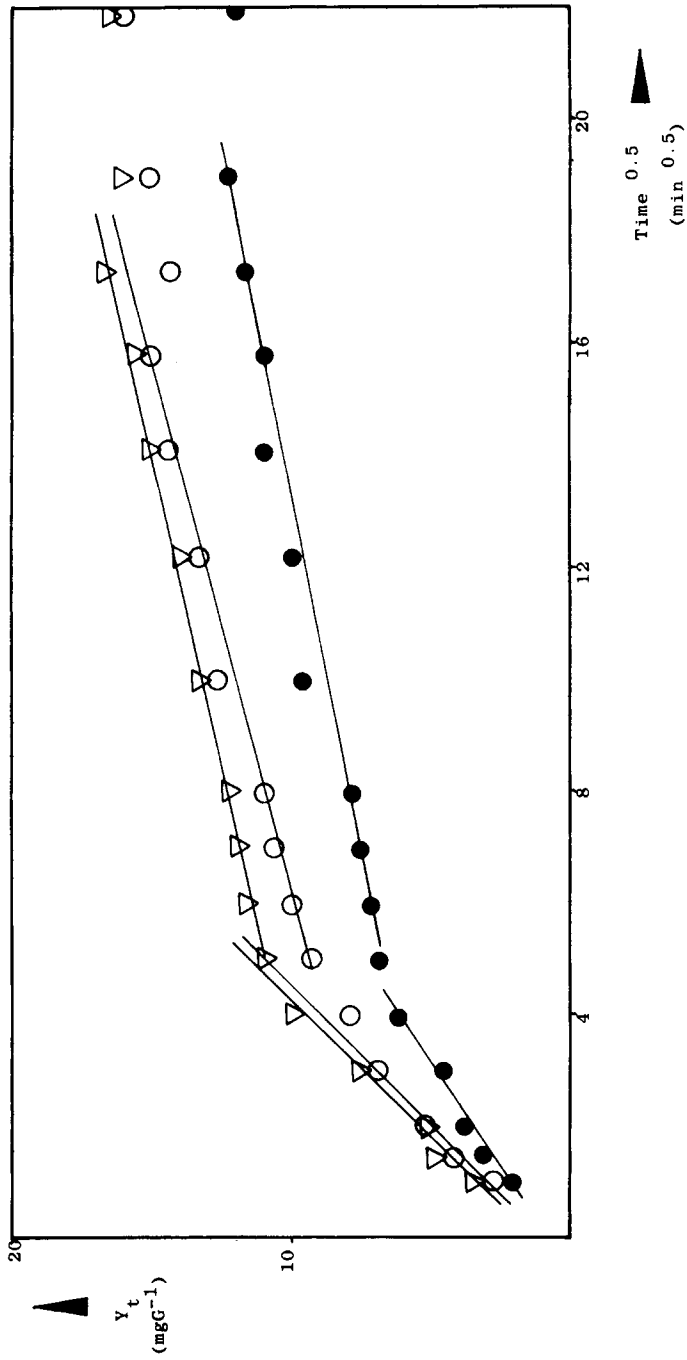


Fig. 4. Intraparticle diffusion dependence for DR 84 (particle size): (▽) 320 μ ; (○) 605 μ ; (●) 925 μ .

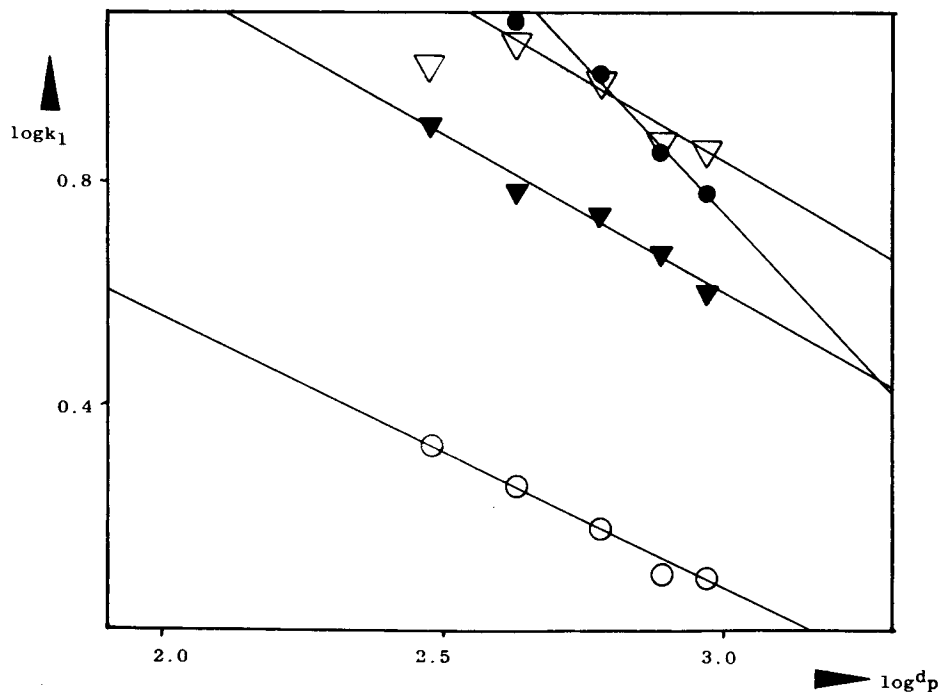


Fig. 5. Variation of $\log k_1$ with $\log d_p$ for the four dyes: (∇) MY 5; (\blacktriangledown) AB 25; (\circ) DR 84; (\bullet) AB 158.

Effect of pH

The variation in k_1 values with pH is reported in Table I for AB 25 and AB 158. Although there was no real pattern, much larger k_1 values were found for both dyes.

It was observed that particle attrition was promoted at the low pH values and this effect was reflected in the increased rate of absorption over longer periods: up to 8 h at pH 2 compared to 2 h for pH 7 and pH 9. This particle size effect was expected to increase the adsorption rate but not the capacity. The increase in the uptake is explained when the physical degradation, brought about by the acidic attack on the chitin chains, is accompanied by H^+ -promoted deacetylation, followed by protonation of the now increased numbers of amine groups. The protonated amine groups constitute a large number of more active sites with formal positive charges for interaction with the dye anions. Well-established isolation techniques involve acid treatments so the leaching of residual H^+ ions into the solution is to be expected, and this increased activity explains the large increase in k_1 values at low pH conditions.

Additional evidence that the internal mass transport requires more than a single rate parameter to describe it completely may be obtained from the branched pore kinetic model.⁸ Work with phenolics separated internal transport into rapidly and slowly diffusing regions, which were associated with macropores and micropores. In the branched pore model, micropores are considered as pores in the range less than 4×10^{-9} m diameter, and, depending on the particular dye and its orientation, the dye molecular diameters vary between 2×10^{-9} m and

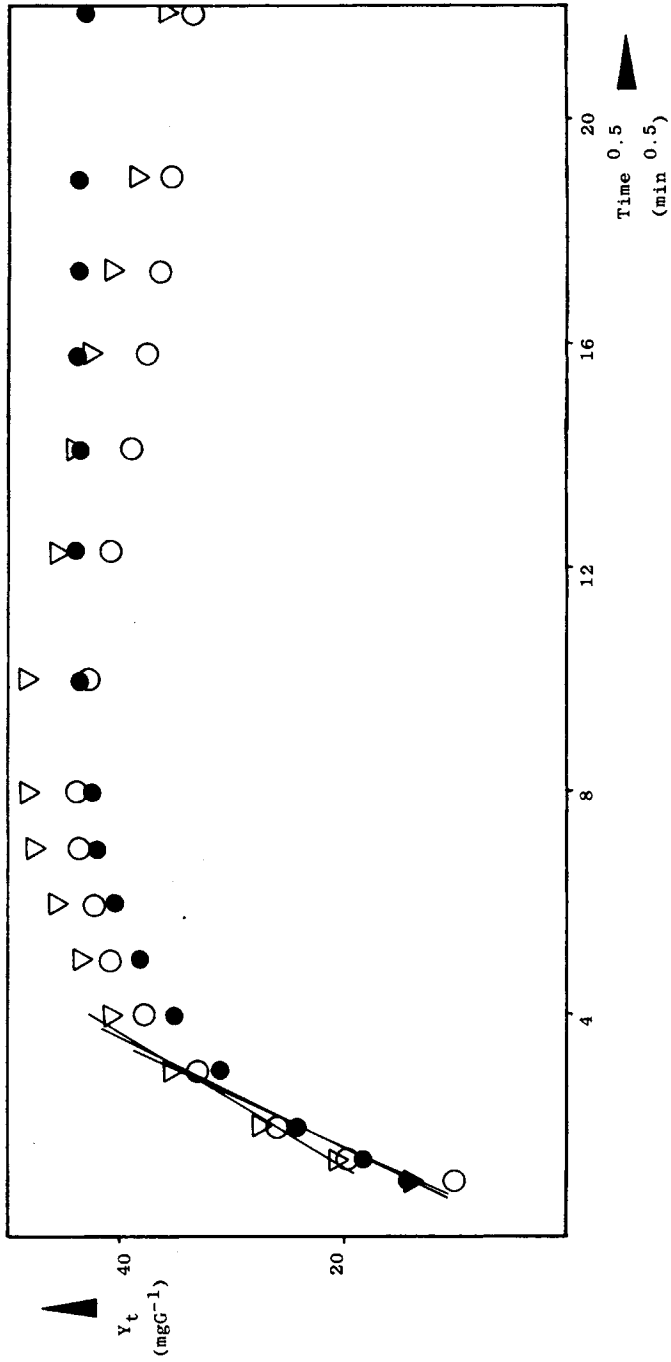


Fig. 6. Intraparticle diffusion dependence for MY 5 (mass): (▽) 2.5 g; (○) 5.0 g; (●) 7.5 g.

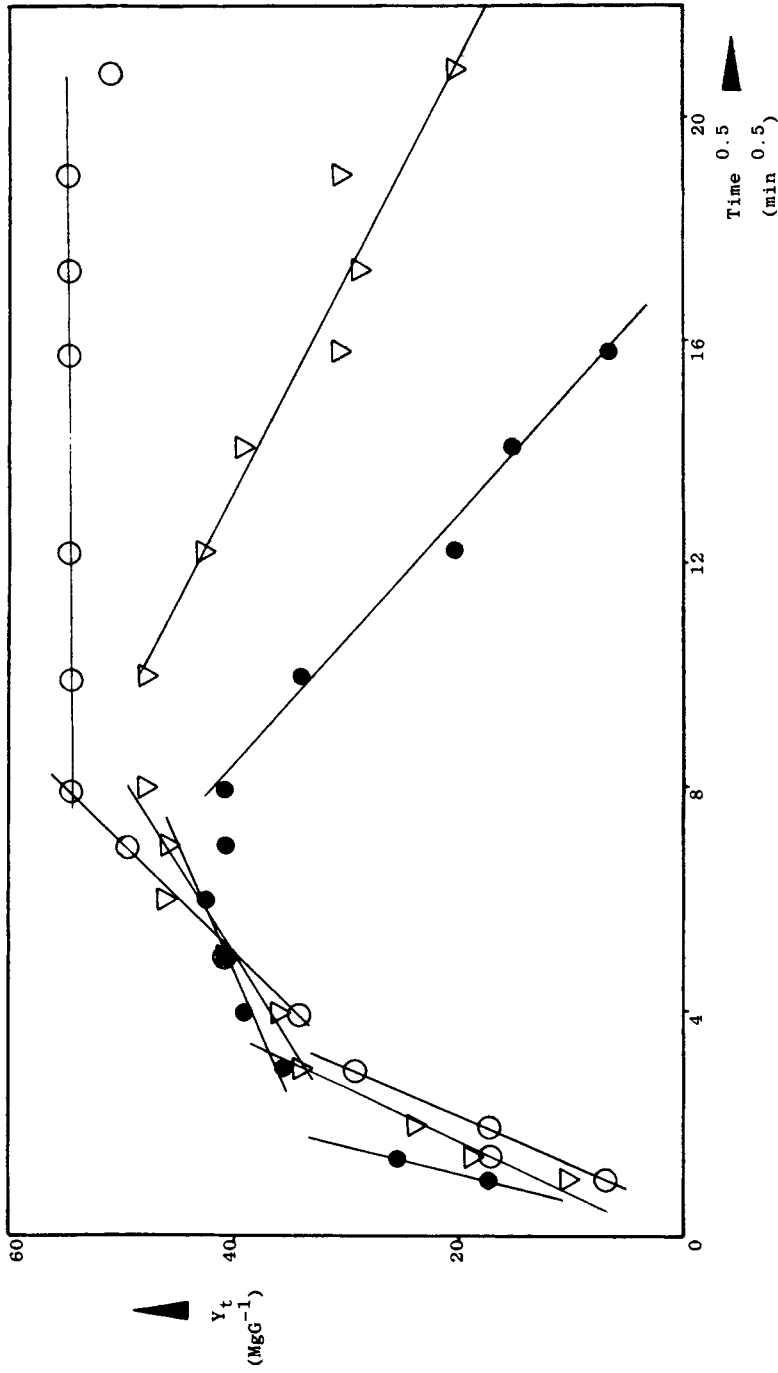


Fig. 7. Intraparticle diffusion dependence for AB 25 (temperature): (○) 30°C; (△) 40°C; (●) 50°C.

20×10^{-9} m; thus there is certainly adsorption into the micropore regions of the chitin particles.

CONCLUSION

Intraparticle diffusion is rate controlling for much of the adsorption process for the adsorption of dyestuffs onto chitin. Initially plots of dye adsorbed against the square root of time are nonlinear, indicating that boundary layer resistance is predominant. However, after this relatively short periods, such plots become linear and are valid for up to several hours depending on the system. The different gradients observed indicate that the internal pore size of the chitin particles offered resistance to dye absorption.

The overall kinetic analysis would need to be based on a more complex two resistance mass transfer model, although the present paper gives a comprehensive model valid for much of the adsorption process.

References

1. G. McKay, H. S. Blair, and J. Gardner, *J. Appl. Polym. Sci.*, **27**, 3043 (1982).
2. G. McKay, H. S. Blair, and J. Gardner, *J. Appl. Polym. Sci.*, **27**, 4251 (1982).
3. J. Crank, *Mathematics of Diffusion*, Clarendon, London, 1965.
4. F. Alexander, V. J. P. Poots, and G. McKay, *Ind. Eng. Chem., Proc. Des. Dev.*, **17**(4), 406 (1978).
5. W. J. Weber and J. C. Morris, *J. Sanit. Eng., Div. Am. Soc. Civ. Eng.*, **90**, 79 (1974).
6. B. A. Bell and A. H. Molof, *Water Res.*, **9**, 857 (1975).
7. M. M. Dubinin, *Proceedings of the Fifth Conference on Carbon*, McMillan, New York, 1962, Vol. 1.
8. R. G. Peel, A. Benedek, and C. M. Crowe, *AIChE J.*, **27**, 26 (1981).

Received July 8, 1982

Accepted November 5, 1982

Corrected proofs received March 11, 1983